

Supplementary Information to

Electron-induced hydroamination of ethane as compared to ethene: Implications for the reaction mechanism

Hannah Boeckers,^a Martin Philipp Mues,^{a,b} Jan Hendrik Bredehöft^a and Petra Swiderek^{*a}

^a Institute for Applied and Physical Chemistry (IAPC), Fachbereich 2 (Chemie/Biologie), University of Bremen, Leobener Str. 5 (NW2), 28359 Bremen, Germany

^b Paderborn University, Institute for Photonic Quantum Systems (PhoQS), Warburger Str. 100, 33098 Paderborn, Germany

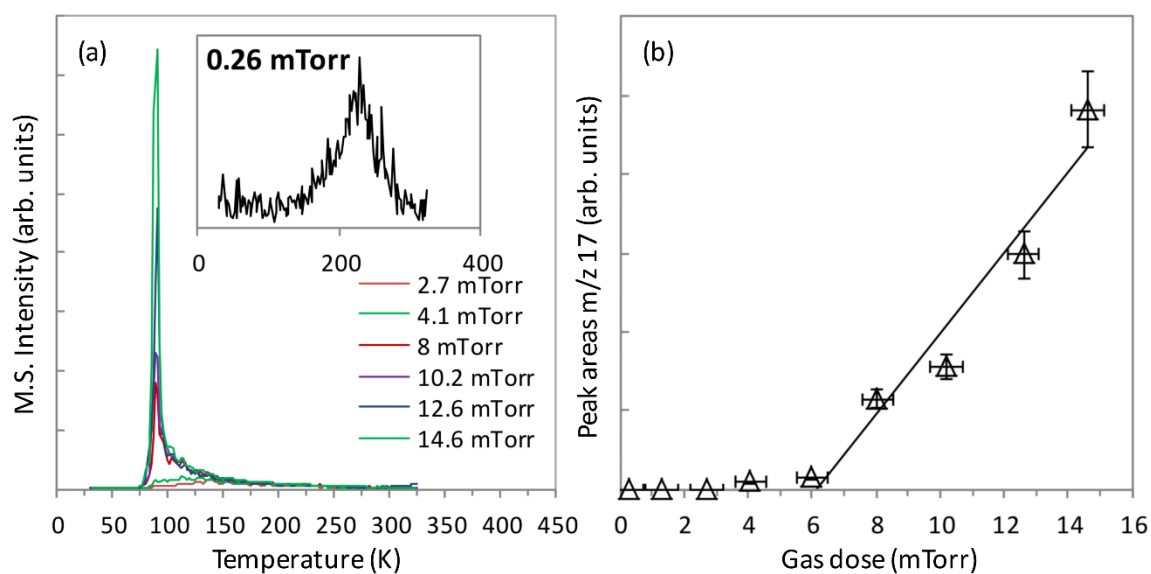


Figure S1. (a) TDS curves obtained for m/z 17 after leaking varying amounts of NH₃ onto the Ta substrate. The gas dose is stated as pressure drop in the gas handing manifold in units of mTorr. (b) Areas of the multilayer desorption peaks ascribed to NH₃ within the m/z 17 TDS curves as function of gas dose obtained by fitting the peaks with a gaussian function [1].

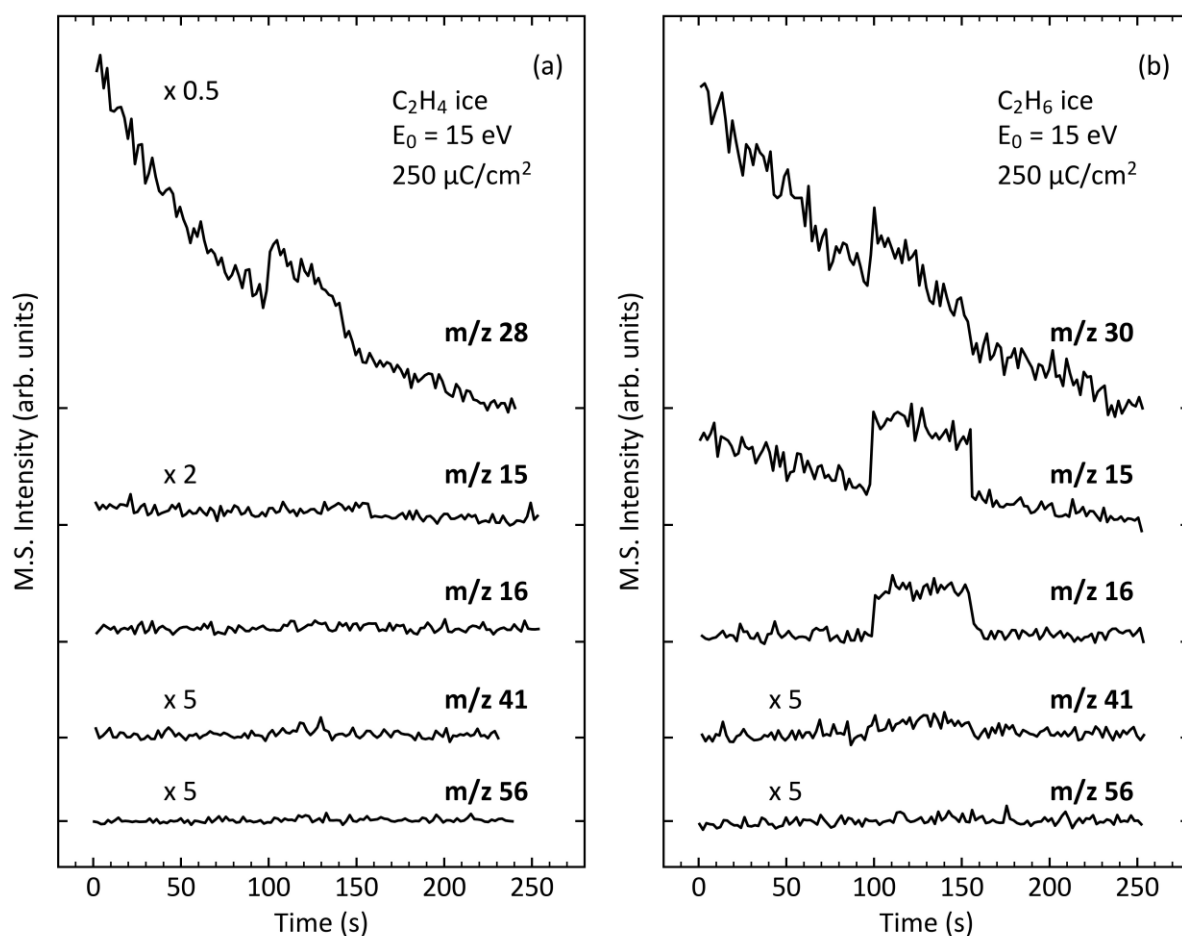


Figure S2. ESD monitored during an electron exposure of $250 \mu\text{C}/\text{cm}^2$ at $E_0 = 15 \text{ eV}$ from (a) C_2H_4 and (b) C_2H_6 ice with an estimated thickness of 10 monolayers. The abrupt increase of the intensity and the sudden decay mark the start and the end of irradiation. The exponential decay of the baseline in the topmost curves relates to the decay of the background pressure of the reactants after leaking into the UHV chamber. The parent signals of C_2H_4 (m/z 28) and C_2H_6 (m/z 30) give evidence of some molecular desorption from the ice. m/z 28 is also the base peak in the mass spectrum (MS) of C_2H_6 while m/z 30 appears only with relative intensity of roughly 30% [2]. m/z 15 appears as fragment in the mass spectrum of C_2H_6 . However, the m/z 16 signal points to electron-induced production of CH_4 from C_2H_6 ice. m/z 41 and m/z 56 are characteristic MS signals of C_4 hydrocarbons (see Table S1). Only m/z 41 carries very small intensity in ESD from C_2H_6 ice indicating that desorption of C_4 products is negligible in line with the lower probability of larger products to desorb and their low abundance after the applied low irradiation doses.

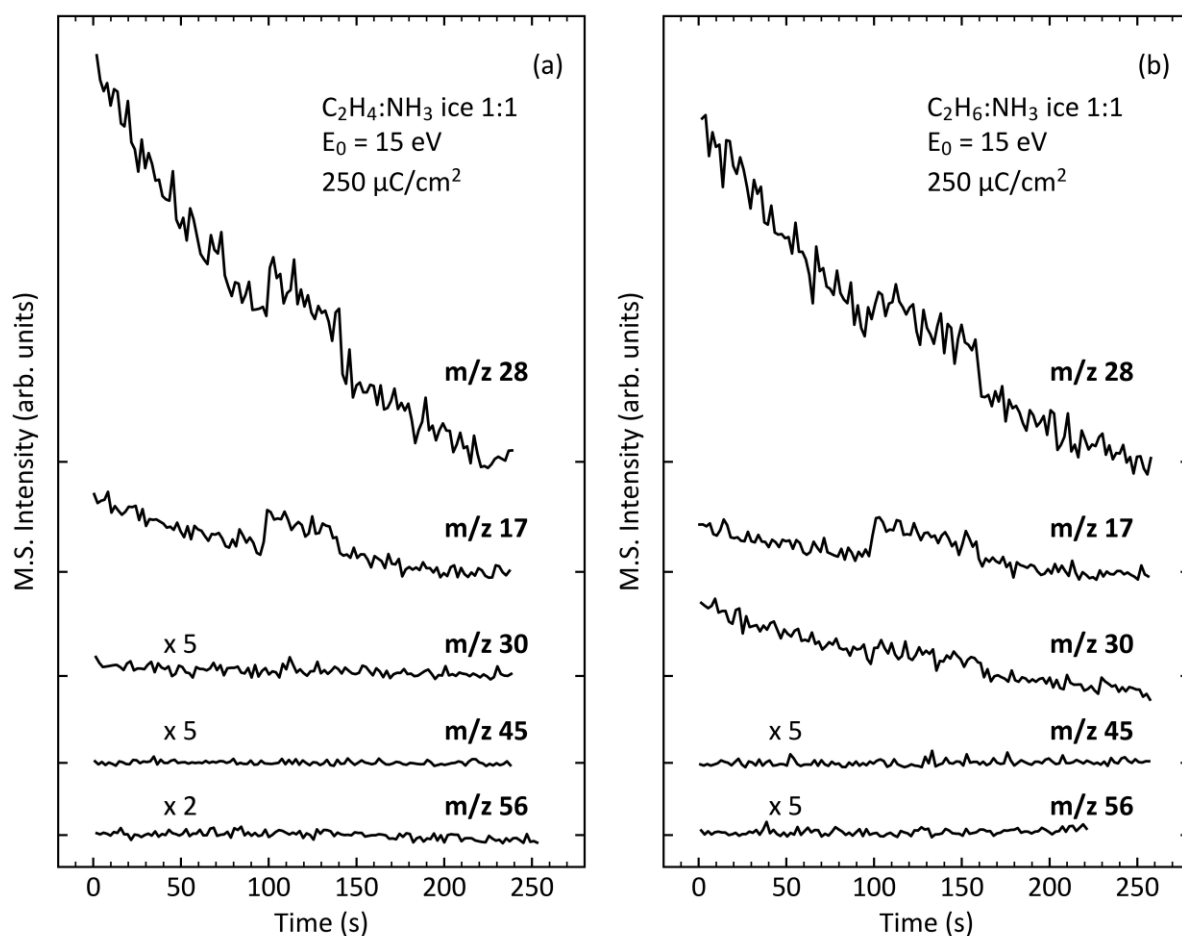


Figure S3. ESD monitored during an electron exposure of $250 \mu C/cm^2$ at $E_0 = 15$ eV from (a) $C_2H_4:NH_3$ and (b) $C_2H_6:NH_3$ ice with an estimated thickness of 10 monolayers. The abrupt increase of the intensity and the sudden decay mark the start and the end of irradiation. The exponential decay of the baseline in the topmost curves relates to the decay of the background pressure of the reactants after leaking into the UHV chamber. The m/z 28 signal can be ascribed to the base signals of C_2H_4 and C_2H_6 but also to N_2 formed as a consequence of electron-induced dissociation of NH_3 [3]. m/z 17 reveals ESD of NH_3 . The parent signal of C_2H_6 (m/z 30) relates to minor molecular desorption of C_2H_6 . m/z 45 is the parent signal of ethylamine and m/z 56 is a characteristic MS signal of C4 hydrocarbons (see Table S1). Both signals do not show evidence for desorption in line with the lower probability of larger products to desorb and their low abundance after the applied low irradiation doses.

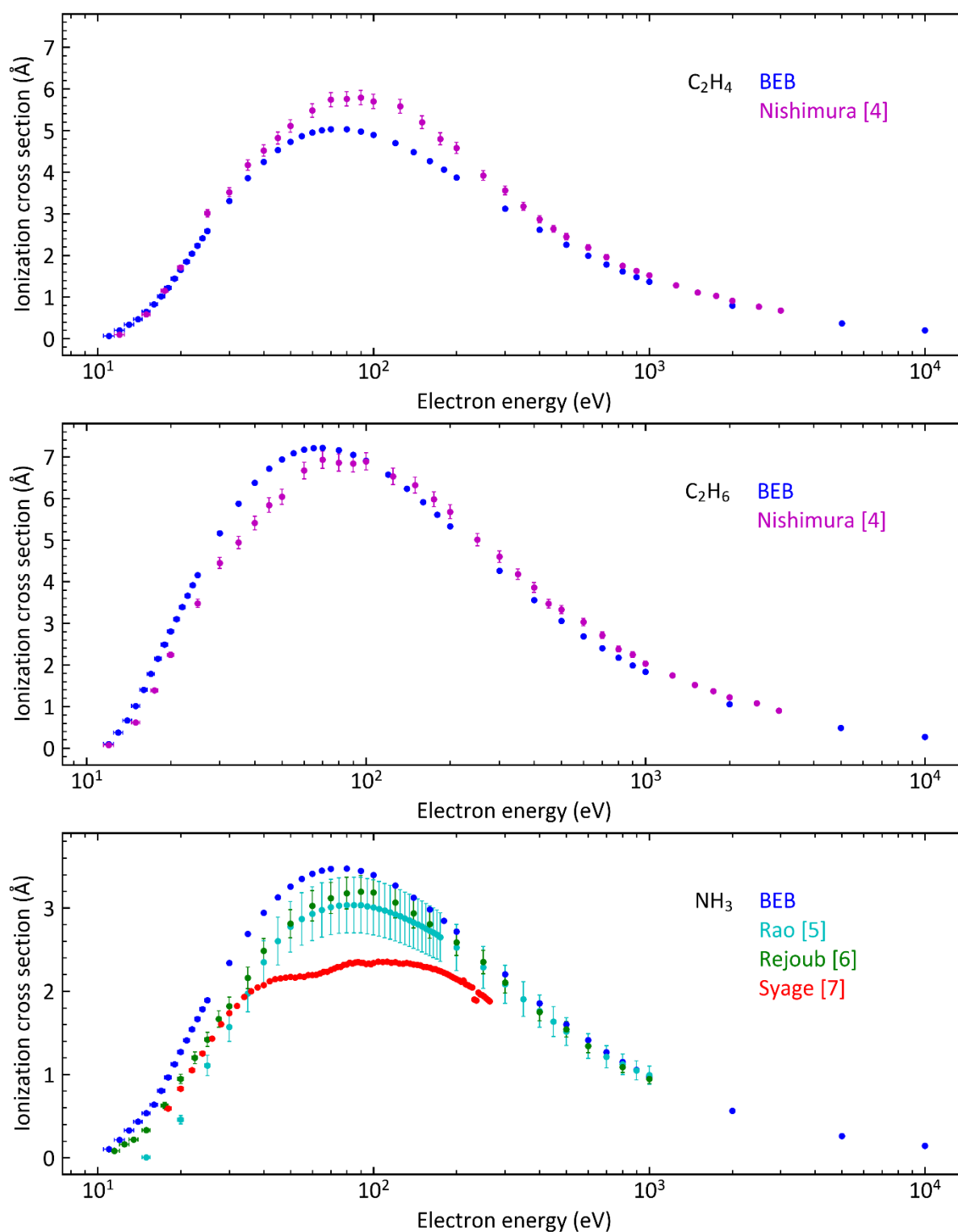


Figure S4. Total electron ionization cross sections (TICS) for C₂H₄, C₂H₆, and NH₃ calculated in the present work (BEB, blue) and comparison to experimental data [4-7]. Note that an estimate of the experimental errors of the data was not provided by Syage [7].

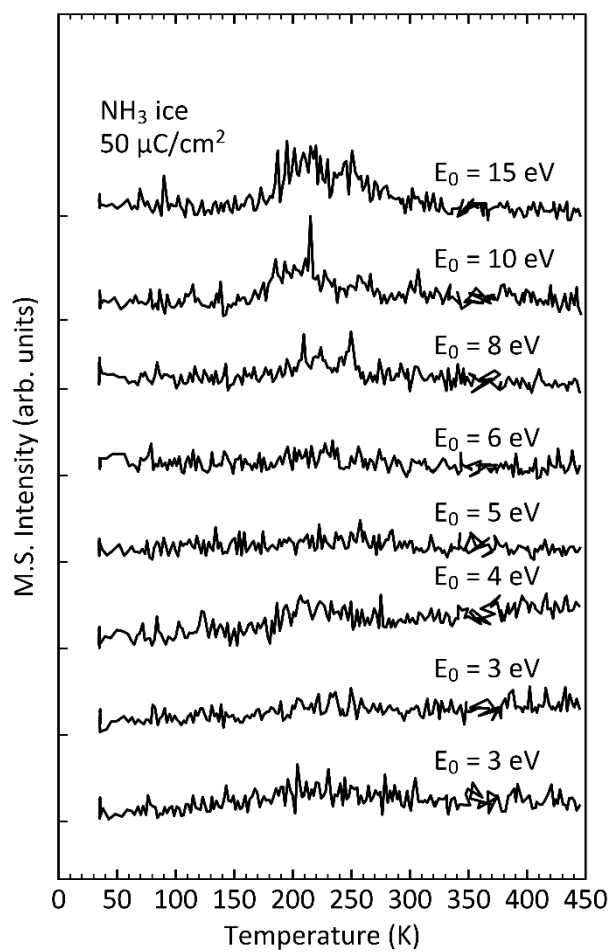


Figure S5. TDS curves obtained for m/z 32 from NH_3 ice with an estimated thickness of 9 monolayers after electron exposure of $50 \mu\text{C}/\text{cm}^2$ at the electron energies stated in the plot.

Table S1. MS intensities for C6 hydrocarbons [2].

C6 hydrocarbon	MS intensities at m/z					
	58	56	54	43	41	39
C ₆ H ₁₄						
n-hexane	4	45	<1	81	70	20
2-methylpentane (isohexane)	<1	4	<1	100	29	13
3-methylpentane	4	77	<1	25	53	9
2,2-dimethylbutane (neohexane)	5	28	<1	100	49	14
2,3-dimethylbutane (diisopropyl)		2	<1	100	45	20
C ₆ H ₁₂						
1-n-hexene	<1	100	5	59	95	31
2-hexene		27	7	14	42	22
2-n-hexene (E)	<1	23	7	12	37	19
2-n-hexene (Z)	<1	25	8	14	50	38
3-n-hexene (E)	<1	28	7	17	81	38
3-n-hexene (Z)		27	6	14	66	24
2-methyl-1-pentene	<1	100	4	10	89	52
3-methyl-1-pentene		44	11	6	75	43
4-methyl-1-pentene (isobutylethene)		50	1	100	68	20
2-methyl-2-pentene	<1	15	2	8	100	19
3-methyl-2-pentene		22	4	8	100	20
3-methyl-2-pentene (E)	<1	21	5	8	100	28
3-methyl-2-pentene (Z)		22	6	6	100	34
4-methyl-2-pentene		8	1	7	100	19
4-methyl-2-pentene (E)	<1	7	2	7	100	28
4-methyl-2-pentene (Z)		7	2	6	100	33
3-methylene-pentane	<1	31	8	10	100	39
2,3-dimethyl-1-butene		7	1	7	100	17
2,3-dimethyl-2-butene		6	1	7	100	18
3,3-dimethyl-1-butene	<1	7	1	4	83	14

Table S1. continued.

C ₆ H ₁₀						
1,3-hexadiene (E)	No NIST data available					
1,3-hexadiene (Z)	No NIST data available					
1,4-hexadiene		2	22	1	51	56
1,4-hexadiene (E)		1	18		40	46
1,4-hexadiene (Z)			17	9	40	43
1,5-hexadiene		<1	59	<1	100	52
2,4-hexadiene		3	17	3	33	24
2,4-hexadiene (E,E)		1	17	<1	36	41
2,4-hexadiene (E,Z)		1	17	<1	35	29
2,4-hexadiene (Z,Z)			15		32	38
2-methyl-1,3-pentadiene		2	17	3	55	61
2-methyl-1,3-pentadiene (E)		2	12		35	41
2-methyl-1,3-pentadiene (Z)	No NIST data available					
3-methyl-1,3-pentadiene (E)		1	13	1	34	38
3-methyl-1,3-pentadiene (Z)			1	12	2	35
4-methyl-1,3-pentadiene	<1	2	14	3	42	30
2-methyl-1,4-pentadiene		2	11	1	41	52
3-methyl-1,4-pentadiene		1	12	1	33	24
2,3-dimethyl-1,3-butadiene		2	32	4	58	57
2-ethyl-1,3-butadiene		7	23	2	50	49
1-hexyne		4	26	42	60	28
2-hexyne		1	36	2	55	62
3-hexyne		2	22	2	88	69
3-methyl-1-pentyne		4	19	1	36	45
4-methyl-1-pentyne	<1	2	12	79	75	33
4-methyl-2-pentyne		1	9	2	93	61
3,3-dimethyl-1-butyne			3		43	31

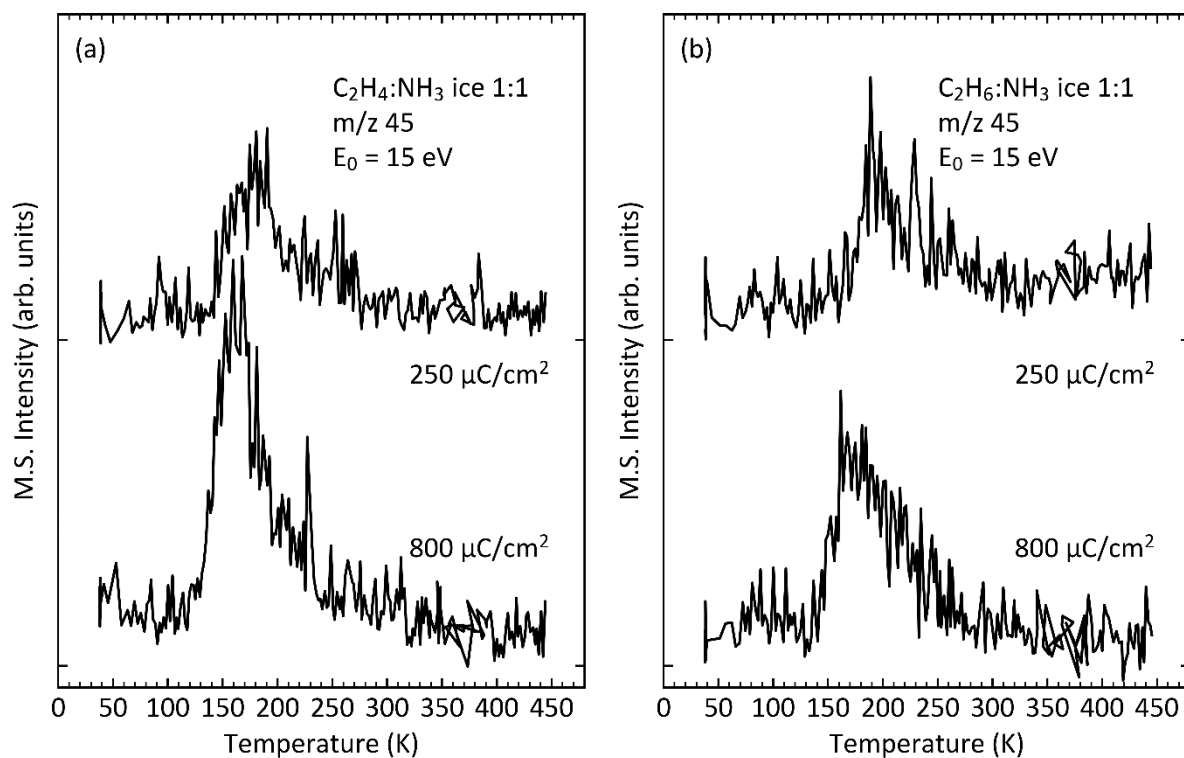


Figure S6. Thermal desorption spectra obtained for m/z 45 from $C_2H_4:NH_3$ (a) and $C_2H_6:NH_3$ (b) ices with an estimated thickness of 12 monolayers after an electron exposure of $250 \mu C/cm^2$ (top) and $800 \mu C/cm^2$ (bottom) at $E_0 = 15 eV$. The vertical axes in both plots are shown with identical magnification with ticks indicating zero intensity for each curve.

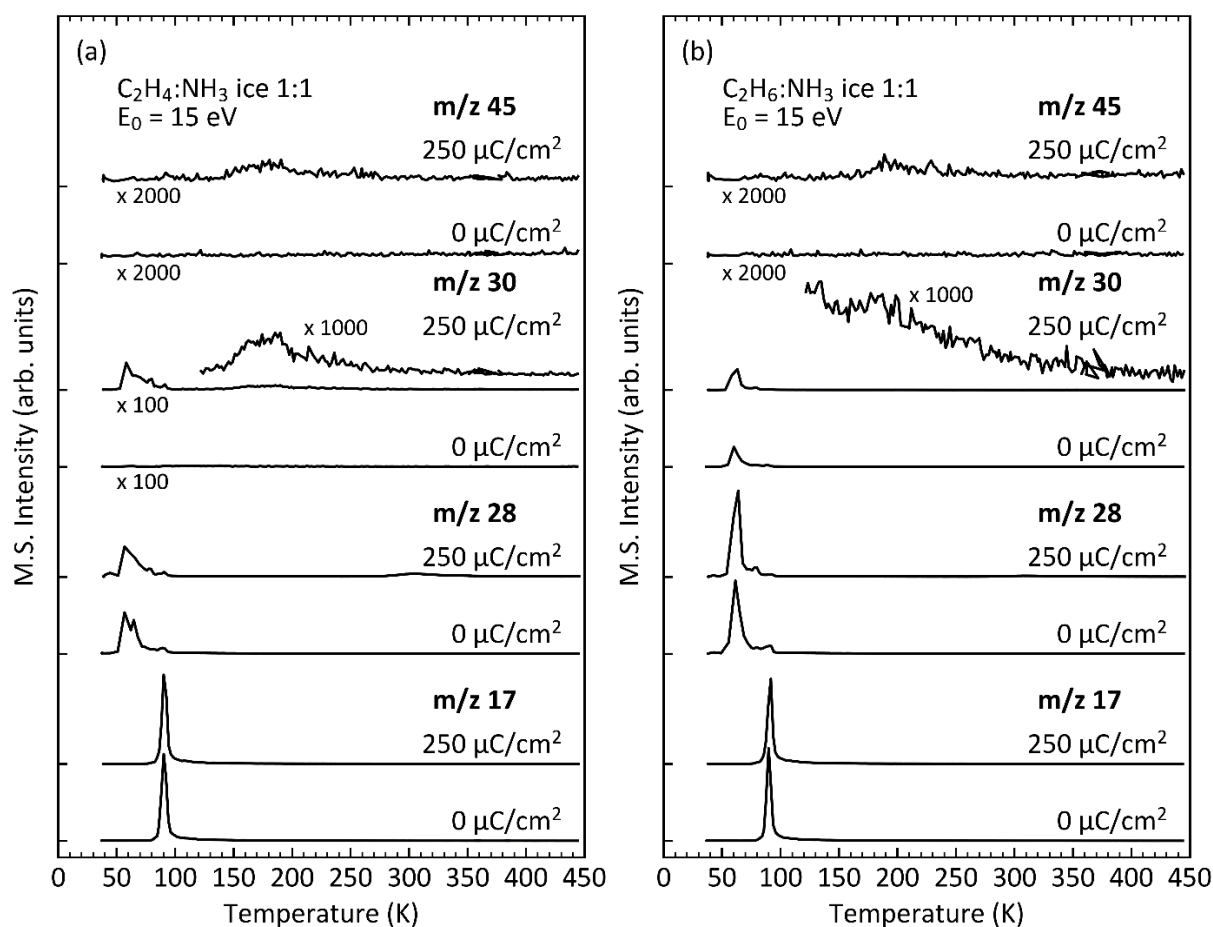


Figure S7. Thermal desorption spectra obtained for m/z 30 (base peak of ethylamine) and m/z 45 (parent signal of ethylamine) as well as m/z 28 (base peak ethane and ethene) and m/z 17 (parent signal NH₃) from (a) C₂H₄:NH₃ and (b) C₂H₆:NH₃ ices (1:1) with an estimated thickness of 12 monolayers without (denoted as 0 μC/cm²) and after an electron exposure of 250 μC/cm² at E₀ = 15 eV. Formation of ethylamine is deduced from the appearance of a desorption signal between 140 K and 200 K after exposure. The vertical axes in both plots are shown with identical magnification with ticks indicating zero intensity for each curve.

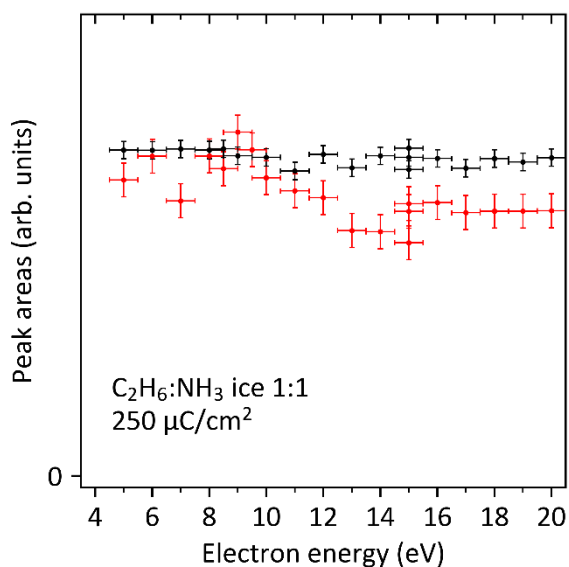


Figure S8. Remaining amounts of C₂H₆ and NH₃ in C₂H₆:NH₃ ices (1:1) with an estimated thickness of 12 monolayers as function of E₀ after an electron exposure of 250 μC/cm². Red symbols represent desorption peak areas derived from TDS curves recorded at m/z 30 which are ascribed to C₂H₆, black symbols represent NH₃ desorption peaks monitored at m/z 17.

References

- [1] Figures adapted with permission from Master Thesis Fabian Schmidt (University of Bremen, 2016).
- [2] Stein, S. E. Mass Spectra. In NIST Chemistry WebBook; NIST Standard Reference Database Number 69; Linstrom, P. J., Mallard, W. G., Eds.; National Institute of Standards and Technology: Gaithersburg, MD; <http://webbook.nist.gov> (accessed 2023-09-11).
- [3] E. Böhler, J. H. Bredehöft and P. Swiderek, *J. Phys. Chem. C*, 2014, **118**, 6922-6933. <https://doi.org/10.1021/jp501192v>
- [4] H. Nishimura and H. Tawara, *J. Phys. B: At. Mol. Opt. Phys.*, 1994, **27**, 2063-2074. DOI 10.1088/0953-4075/27/10/016
- [5] M. V. V. S. Rao and S. K. Srivastava, *J. Phys. B: At. Mol. Opt. Phys.* 1992, **25**, 2175-2187. DOI 10.1088/0953-4075/25/9/021
- [6] R. Rejoub, B.G. Lindsay and R.F. Stebbings, *J. Chem. Phys.* 2001, **115**, 5053-5058. <https://doi.org/10.1063/1.1394748>
- [7] J.A. Syage, *Aerospace Report No. TR-94(4231)-3*, 1994. <https://apps.dtic.mil/sti/pdfs/ADA281248.pdf>